Cancer Cell
Article

A Two-in-One Antibody against HER3 and EGFR Has Superior Inhibitory Activity Compared with Monospecific Antibodies

Gabriele Schaefer,[1,7] Lauric Haber,[2,7] Lisa M. Crocker,[3] Steven Shia,[4] Lily Shao,[1] Donald Dowbenko,[1] Klara Totpal,[3] Anne Wong,[5] Chingwei V. Lee,[2] Scott Stawicki,[2] Robyn Clark,[3] Carter Fields,[1] Gail D. Lewis Phillips,[1] Rodney A. Prell,[6] Dimitry M. Danilenko,[6] Yvonne Franke,[4] Jean-Philippe Stephan,[5] Jiyoung Hwang,[4] Yan Wu,[2] Jenny Bostrom,[2] Mark X. Sliwkowski,[1,*] Germaine Fuh,[2,*] and Charles Eigenbrot[2,4,*]
[1]Department of Research Oncology
[2]Department of Antibody Engineering
[3]Department of Translational Oncology
[4]Department of Structural Biology
[5]Department of Assay Automation Technology
[6]Department of Safety Assessment
Genentech, Inc., South San Francisco, CA 94080, USA
[7]These authors contributed equally to this work
*Correspondence: marks@gene.com (M.X.S.), fuh.germaine@gene.com (G.F.), eigenbrot.c@gene.com (C.E.)
DOI 10.1016/j.ccr.2011.09.003

SUMMARY

Extensive crosstalk among ErbB/HER receptors suggests that blocking signaling from more than one family member may be essential to effectively treat cancer and limit drug resistance. We generated a conventional IgG molecule MEHD7945A with dual HER3/EGFR specificity by phage display engineering and used structural and mutational studies to understand how a single antigen recognition surface binds two epitopes with high affinity. As a human IgG1, MEHD7945A exhibited dual action by inhibiting EGFR- and HER3-mediated signaling in vitro and in vivo and the ability to engage immune effector functions. Compared with monospecific anti-HER antibodies, MEHD7945A was more broadly efficacious in multiple tumor models, showing that combined inhibition of EGFR and HER3 with a single antibody is beneficial.

INTRODUCTION

Deregulation of the epidermal growth factor receptor family plays an important role in tumorigenesis (Hynes and MacDonald, 2009), and targeted agents directed against two members of the HER/ErbB family, epidermal growth factor receptor (EGFR/HER1) and HER2/ErbB2, are used in the treatment of cancer (Ciardiello and Tortora, 2008; Moasser, 2007). Mutation and/or overexpression of these receptors produce aberrant proliferative signals arising from the tyrosine kinase activity of their intracellular domains. There is promiscuous association among family members and each receptor activates a distinct but overlapping repertoire of downstream pathway components (Jones et al., 2006; Olayioye et al., 2000) and multiple receptors can contribute to tumor growth.

To date, HER3 is not reported to undergo oncogenic activation as a result of mutation or amplification. However, during the last decade unique structural aspects of HER3 emerged which produced insights and questions regarding the receptor's function in normal tissue and hyperproliferative conditions such as cancer. The cognate ligand for HER3 is heregulin (HRG; also called neu differentiation factor) (Carraway et al., 1994). In the absence of an appropriate coreceptor, HRG binds to HER3 with relatively low affinity. In the presence of another HER family member, the low-affinity HRG binding site is converted to a high-affinity site by the formation of a heterodimeric complex

Significance

Alterations in expression or activation of HER/ErbB family members can limit the efficacy or lead to resistance to monospecific antibodies targeting individual ErbB/HER receptors. A two-in-one antibody, MEHD7945A, binds to EGFR and HER3/ErbB3 and inhibits receptor function. Here, we demonstrate superiority of the dual-specific EGFR/HER3 antibody to monospecific HER antibodies. The activity profile of the dual-specific EGFR/HER3 antibody validates the utility of simultaneously targeting both receptors and supports its clinical evaluation in settings where HER/ErbB signaling is thought to play a major role in tumorigenesis.

(Sliwkowski et al., 1994). Additionally, the HER3 extracellular domain exists in a closed conformation and undergoes an impressive conformational change in the presence of ligand that allows for the formation of a two domain ligand binding site and the exposure of a receptor dimerization arm (Cho and Leahy, 2002). Because it is a pseudokinase (Jura et al., 2009b), HER3 was initially, and simplistically, regarded as being merely a substrate for HER/ErbB transactivation. Recent, elegant studies further elaborate the HER3 kinase domain as an allosteric activator for its enzymatically competent counterparts (Jura et al., 2009a). HER3 is further differentiated from other HER family members, and for that matter other receptor tyrosine kinases, by the presence of six tyrosines in the C-terminal tail that when phosphorylated directly recruit the p85 subunit PI3 kinase (Prigent and Gullick, 1994; Soltoff et al., 1994). As a consequence, the HER3-PI3 kinase node is emerging as a potential target for anticancer therapy (Schoeberl et al., 2010).

The therapeutic EGFR antibodies cetuximab and panitumumab antagonize EGFR signaling by blocking ligand binding. These antibodies show marginal objective responses in advanced colorectal cancer patients when used as single agents. Randomized trials of EGFR antibodies combined with chemotherapy showed a statistically significant, albeit modest, increase in progression free survival versus chemotherapy alone, especially in tumors that are wild-type for K-ras (Grothey, 2010).

The most impressive single agent activity of EGFR antagonists is observed in non-small cell lung cancer (NSCLC) patients whose tumors harbor somatic kinase domain mutations and are treated with erlotinib or gefitinib (Lynch et al., 2004; Paez et al., 2004). In contrast, the clinical benefit in patients with wild-type EGFR NSCLC is considerably diminished. Preclinical studies report a strong association between sensitivity to gefitinib in NSCLC cell lines and the inactivation of HER3 (Engelman et al., 2005). Moreover, this observation was extended to a panel of colorectal and pancreatic cancer cell lines, where erlotinib antiproliferative activity was again correlated with inhibition of HER3 phosphorylation (Buck et al., 2006). These findings raise the possibility that in the absence of EGFR kinase domain mutations, optimal clinical benefit of anti-EGFR requires that HER3 is also inhibited.

Antibodies are valued as therapeutics for their high affinity and exquisite specificity. To further build on this clinical success, a wide array of proteins with antibody-like binding properties is now available. For example, the generation of many bispecific platforms, which vary from small diabody formats to tetrameric structures (Chames and Baty, 2009). Antibodies engineered with more than one binding specificity enable multiple antigens to be targeted, for example, EGFR and the T cell receptor (Lutterbuese et al., 2010). Typically, these bitargeting agents are constructed by linking two distinct antigen-binding modules into one molecule, each module being able to bind only one antigen. We reasoned that a combination of an antibody directed against EGFR and HER3 might be more effective for EGFR-driven cancers than existing antibody therapies. Our approach was to double the function of a single antibody binding site creating a surface that specifically binds two, and only two, target antigens with high affinity. This notion is a stark violation of a cardinal property of natural antibodies, that one antibody recognizes one, and only one antigen. The first such two-in-one antibody described binds VEGF and HER2 (Bostrom et al., 2009). Our aim in the current work was to generate a two-in-one antibody directed against HER3 and EGFR.

RESULTS

Complete Inhibition of MAPK and AKT Signaling Is Achieved Only When EGFR and HER3 Are Blocked Simultaneously

The two major downstream signaling pathways in the HER/ErbB family activated in response to ligand stimulation are the Ras/MAPK and the phosphatidylinositol 3-kinase (PI3K)/AKT pathway. To learn if the blockade of either EGFR or HER3 alone is sufficient to inhibit both pathways, we evaluated pathway modulation using ligands and antireceptor antibodies. We chose two cell lines that express similar levels of HER3 but differ greatly in EGFR expression to better reflect the variations of receptor levels seen in tumor cells: A431 cells ($\sim$1.2 $\times$ 10^6 EGFR per cell) and BxPC3 cells ($\sim$6.3 $\times$ 10^4 EGFR per cell) (Lynch and Yang, 2002). Treatment with the HER3 ligand heregulin (HRG) induced robust phosphorylation of HER3 and AKT in both cell lines but had no effect on EGFR phosphorylation and only marginal effect on ERK1/2 phosphorylation (Figure 1, lane 2). The phosphorylation of HER3 and AKT was ablated when cells were pretreated with an anti-HER3 antibody (lane 3) but were unchanged when treated with cetuximab (lane 4). In contrast, treatment with the EGFR ligand TGF-α resulted in strong phosphorylation of EGFR and ERK1/2 but had no or marginal effect on HER3 or AKT phosphorylation (lane 5). Pretreatment with cetuximab effectively blocked TGF-α-induced phosphorylation of EGFR and ERK1/2 (lane 7), whereas anti-HER3 had no effect (lane 6). Importantly, in the presence of both ligands robust phosphorylation of HER3, EGFR, AKT and ERK1/2 occurred (lane 8) and only pretreatment with cetuximab plus anti-HER3 completely prevented receptor phosphorylation and downstream signaling in both cell lines (lane 11). These findings suggest that, in a ligand-rich tumor environment, effective shutdown of the HER axis would require ablation of both EGFR- and HER3-driven signaling.

Generation of a Ligand Blocking Anti-EGFR Monoclonal Antibody

To explore the therapeutic potential of a dual-action antibody that can block both signaling pathways, we sought to generate an antibody that would recognize and inhibit EGFR as well as HER3. We first isolated an anti-EGFR antibody, D1, from a phage-displayed Fab library based on its ability to block TGF-α binding to EGFR and then improved D1 to the high-affinity variant D1.5 (K_d = 0.4 nM) by affinity maturation (Lee et al., 2006; Figure 2A). D1.5 potently inhibited ^{125}I-EGF binding to EGFR (Figure S1). The ability of D1.5 to block ligand binding translated into potent inhibition of TGF-α-stimulated phosphorylation of EGFR, downstream signaling, and cell proliferation of EGFR-NR6 cells. Further, D1.5 demonstrated potent antitumor activity in the EGFR amplified A431 xenograft model that is highly sensitive to anti-EGFR therapeutics (Figure 2B and Figure S1). The antitumor activity of D1.5 was comparable to the activity seen with cetuximab (K_d = 0.7 nM) (Table S1).

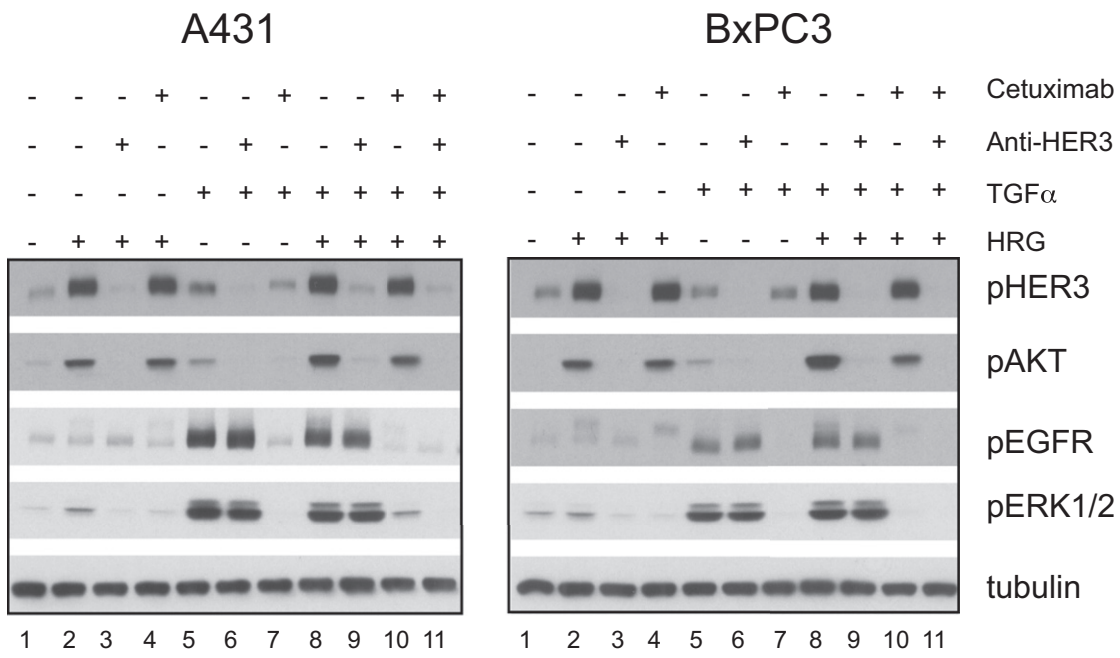

Figure 1. Combination of EGFR and HER3 Antibodies Is Necessary to Abolish Ligand Induced Activation of PI3K/AKT and ERK Signaling
A431 and BxPC3 cells were treated for 3 hr with indicated antibodies (10 μg/ml) and stimulated with HRG (0.5 nM), TGF-α (0.5 nM), or combination of both ligands for 10 min. Cell lysates were immunoblotted to detect pHER3 (Tyr1289), pAKT (Ser473), pERK1/2 (Thr202/Tyr204), pEGFR (Tyr1068), and tubulin.

Addition of HER3 Binding to the Anti-EGFR Antibody

After establishing D1.5 as an effective EGFR inhibitor, we sought to add anti-HER3 activity. Since D1.5 was isolated from an antibody library with diversity restricted to the heavy-chain CDRs, we expected its important anti-EGFR residues to be in the heavy chain. We constructed a library of D1.5 variants with mutations in the light-chain CDRs and were able to identify clones that bound HER3 while maintaining binding to EGFR. These clones, e.g., D1.5-100, not only bound to both receptors but also blocked ligand binding to EGFR and HER3, albeit with much reduced affinity for EGFR (EC_{50} ~100 nM) (Figure 2A).

To demonstrate antiproliferative activity of these dual-specific antibodies, we reformatted and expressed several phage clones as human IgG1 proteins. To evaluate HER3 inhibition, we chose a breast cancer cell line, MDA-MB-175, that secretes HRG and as a result activates HER3 in an autocrine manner (Schaefer et al., 1997). We used EGFR-NR6 cells as described above to verify the antagonism of EGFR. As expected, D1.5 potently inhibited ligand-induced growth of EGFR-NR6 cells in a dose-dependent manner but had no effect on the growth of MDA-MB-175 cells (Figure 2B). The dual-specific antibodies, however, were able to inhibit EGFR- and HER3-mediated proliferation in the two cell lines. D1.5-100, which differs from D1.5 by only five amino acid substitutions in the light chain (Figure 2A), potently inhibited the growth of MDA-MB-175 cells, demonstrating that binding to HER3 translated into potent in vitro activity. However, the low affinity of D1.5-100 for EGFR led to inhibition of TGF-α-driven growth of EGFR-NR6 cells only at high concentrations (Figure 2B).

To improve the dual affinity of D1.5-100, we first assessed the energetic importance of the CDR residues necessary for binding to EGFR and HER3 using alanine and homolog mutagenesis scanning (Supplemental Experimental Procedures). The analysis revealed that, as expected, heavy-chain CDR residues are dominant in EGFR binding. In contrast, HER3 binding required residues from both light-chain and heavy-chain CDRs (Table S2). By stringent affinity-based selection from the homolog libraries, we identified many variants with improved affinity. We focused on one Fab, designated DL11f (termed MEHD7945A when reformatted as IgG), which exhibited improved binding affinities for both EGFR and HER3 (K_d 1.9 and 0.4 nM, respectively) (Figure 2A, Table S1). DL11f has twelve amino acid substitutions compared with D1.5. The enhanced binding affinities of DL11f for EGFR and HER3 translated into increased antiproliferative activity in EGFR-NR6 and MDA-MB-175 cells (Figure 2B).

EGFR and HER3 Compete for Binding to MEHD7945A

To assess specificity, we examined the binding of DL11f toward a panel of proteins using an ELISA assay. As expected, DL11f bound to human EGFR and human HER3. Interestingly, DL11f cross-reacted with murine EGFR but not with murine HER3; both orthologs are highly homologous to the human counterpart. DL11f did not show any detectable binding to HER2 or HER4 (data not shown).

Typically, bitargeting agents are constructed by linking two distinct antigen-binding modules, each module being able to bind to only one antigen. In contrast, in MEHD7945A, each module (Fab) can bind either of two antigens, thus having the potential to elicit enhanced binding affinity from an avidity effect. To confirm that each of the two identical Fabs of MEHD7945A can bind either EGFR or HER3, we performed a competitive binding assay. MEHD7945A binding to immobilized HER3-ECD

A

	CDR L1						CDR L2				CDR L3						Phage EC50 (nM)		Fab Kd (nM)	
	28	29	30	31	32	33	50	51	52	53	91	92	93	94	95	96	EGFR	HER3	EGFR	HER3
D1	D	V	S	T	A	V	S	A	S	F	S	Y	T	T	P	P	>1000	NB	nd	nd
D1.5	D	V	S	T	A	V	S	A	S	F	S	Y	P	T	P	Y	1	NB	0.4	NB
D1.5-100	D	L	A	T	D	V	S	A	S	F	S	E	P	E	P	Y	112.9	2	nd	nd
DL11	D	L	A	T	D	V	S	A	S	F	S	E	P	E	P	Y	3.7	0.5	nd	nd
DL11f	N	I	A	T	D	V	S	A	S	F	S	E	P	E	P	Y	2.5	0.3	1.9	0.4

	CDR H1						CDR H2									CDR H3										
	29	30	31	32	33	48	50	51	52	52a	53	54	55	56	57	58	95	96	97	98	99	100	100a	100b	100c	101	102	103
D1	F	T	G	N	W	V	E	I	S	P	S	G	G	Y	T	D	E	S	R	V	S	Y	E	A	A	M	D	Y
D1.5	F	T	G	N	W	V	E	I	S	P	S	G	G	Y	T	D	E	S	R	V	S	Y	E	A	A	M	D	Y
D1.5-100	F	T	G	N	W	V	E	I	S	P	S	G	G	Y	T	D	E	S	R	V	S	Y	E	A	A	M	D	Y
DL11	L	S	G	D	W	L	E	I	S	A	A	G	G	Y	T	D	E	S	R	V	S	F	E	A	A	M	D	Y
DL11f	L	S	G	D	W	V	E	I	S	A	A	G	G	Y	T	D	E	S	R	V	S	F	E	A	A	M	D	Y

B

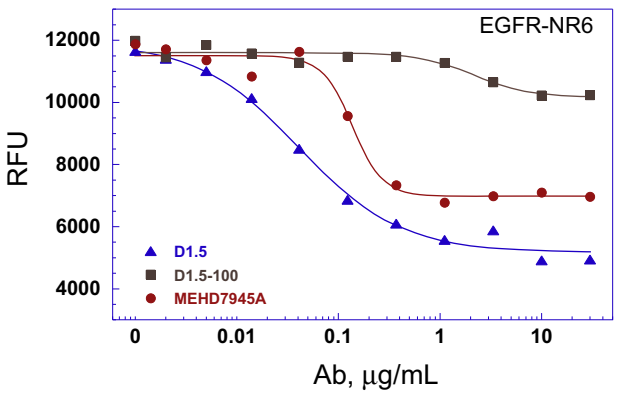

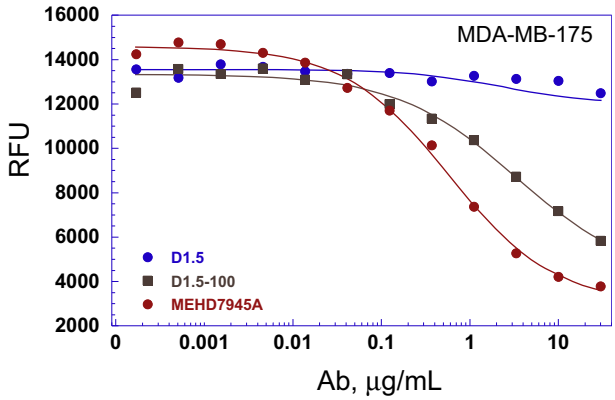

C

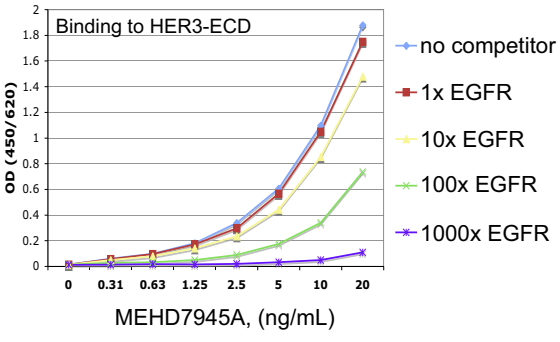

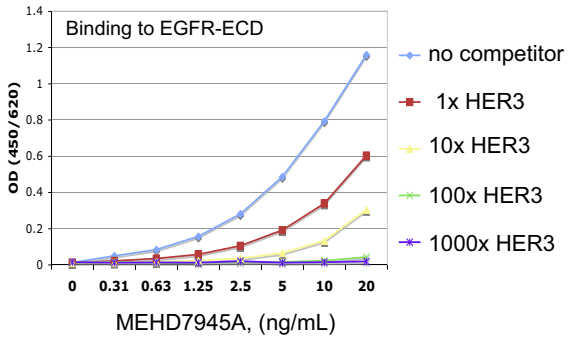

Figure 2. Biochemical Characterization of the Dual-Action Antibodies and Their Monospecific Parents

(A) Sequence alignment of CDRs of D.1, D1.5, D1.5-100, DL11, or DL11f, in the order they were created. Amino acid changes relative to each sequence's immediate precursor are highlighted in yellow. Relative affinities of the various Fabs as phage clones or as purified Fab protein were determined by ELISA or SPR, respectively.

(B) EGR-NR6 cells in the presence of 3 nM TGF-α, or MDA-MB-175 cells were treated with indicated concentrations of D1.5 (blue line), D1.5-100 (gray line), or MEHD7945A (red line) in the presence of 1% serum containing growth medium. Cell proliferation was measured after 3 days using AlamarBlue staining. The results are expressed in relative fluorescence units (RFU).

(C) MEHD7945A binding to immobilized HER3-ECD or EGFR-ECD as indicated in the presence of indicated soluble competitor. 1× = 0.02 µg/ml, 10× = 0.2 µg/ml, 100× = 2 µg/ml, 1000× = 20 µg/ml. Results expressed as MEHD7945A concentration versus OD.

See also Figure S1 and Tables S1 and S2.

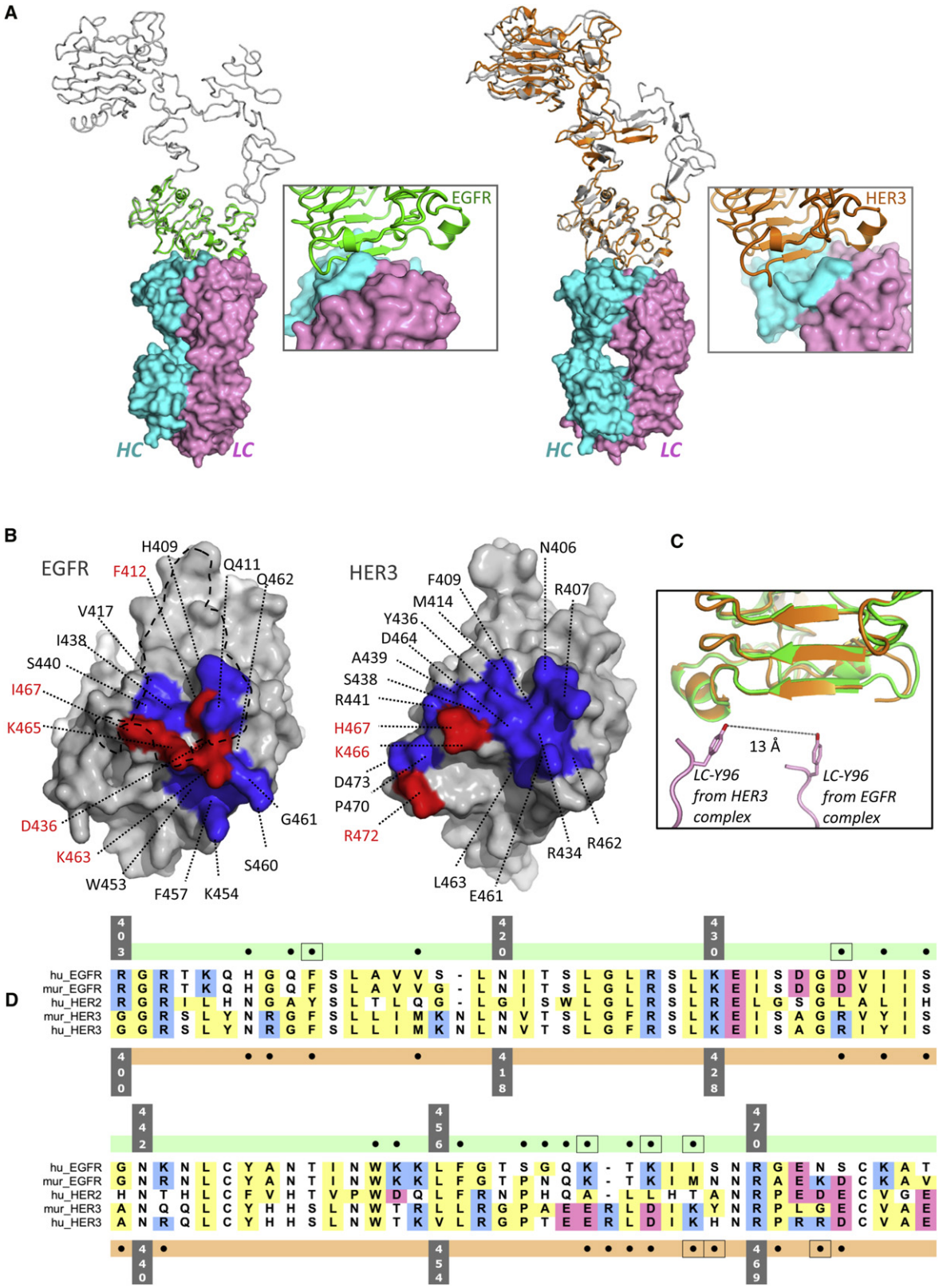

Figure 3. Crystal Structure of DL11 in Complex With EGFR-ECD or HER3-ECD

(A) DL11 (surface in pink [light chain] and blue [heavy chain]) binds to EGFR (left, green) and to HER3 (right, orange) at similar regions of domains 3. The magnified views (boxed) are viewed after aligning EGFR and HER3 domain 3. For EGFR, the full-length version of EGFR ecd found in PDB entry 1YY9 is included for

was reduced in a dose-dependent manner with increasing amounts of EGFR-ECD. Conversely, MEHD7945A was competed from immobilized EGFR-ECD by soluble HER3-ECD protein. As expected, given their relative binding constants, higher concentrations of soluble EGFR-ECD were needed to compete with binding of MEHD7945A to immobilized HER3-ECD (Figure 2C).

Key Differences in the Way DL11 Binds EGFR and HER3

To learn how a single Fab interacts with two homologous receptors (homology in ECD 45%), we determined crystallographic structures of DL11 alone (2.85 Å), in complex with EGFR domain 3 (residues Arg310-Lys514) (1.8 Å) and in complex with HER3 domains 1–3 (residues Ser1-His513) (3.7 Å) (Figure 3, Table S3). DL11 is a variant of DL11f differing by three subtle amino acid differences (Figure 2A) with indistinguishable binding (Table S1) and antiproliferative activities (data not shown). DL11 Fabs in the three structures have no significant differences in their main chain conformations (Figure S2). The arrangement of the HER3 domains 1–3 in the HER3-DL11 complex is essentially identical to the "tethered" structure of unliganded HER3 (Cho and Leahy, 2002; Figure 3A).

The sizes of the DL11/receptor interfaces are typical for antibody-protein antigen complexes, with the EGFR complex having 800 $Å^2$ buried on each side, and the HER3 complex having 890 $Å^2$. The larger interface area in the HER3 complex arises from the inclusion of twice as much DL11 light-chain surface as in the EGFR complex (225 versus 100 $Å^2$) (Figure 3A). This is consistent with the greater importance of light-chain CDR residues for HER3 binding (Table S4) and the fact that HER3 binding was initially acquired using changes in the light chain of D1.5.

The DL11 epitopes are at similar region of domain 3 of the two receptors but are shifted with respect to each other by 13 Å (Figures 3A and 3C). The shift of the structural epitopes is revealed by the distinct sets of main contacts, which are at a segment of low homology (Figure 3D). Although the epitopes on the two receptors do not exactly correspond to each other structurally, there are some common features in the two interfaces: both epitopes are generally basic and the antibody contact regions are generally acidic (Figure S2).

The EGFR epitope of DL11 overlaps with the cetuximab epitope and they both include ligand-binding residues (Li et al., 2005, Figure 3B, Figure S2). In addition, both antibodies would present a steric clash limiting the receptor's access to the "untethered" conformation that is stabilized by ligand binding (Figure S2). Such a conformation is implicated in receptor signaling. At present, there is no crystal structure reported for HER3 bound to a ligand, but we presume HER3 ligands bind regions on domain 1 and domain 3 by analogy to EGFR/ligand structures. Thus, the DL11f mechanism of action for both EGFR and HER3 is one of ligand blocking and a restriction on ECD conformations.

We next performed alanine scanning of both receptors to determine the energetic contributions of the residues making structural contacts (Figure 3B, Figure S2). We found that residues in the center of the contact regions and their interacting residues on DL11 are generally important functionally thus corroborating the crystal structures (Figure 3B). The critical importance of Arg472 and His467 for the HER3 interaction explains why DL11f does not bind murine HER3 as the two residues are not conserved in murine HER3, which is otherwise 94% identical to human HER3 (Figure 3D). Consistent with the polar natures of the interacting surfaces, the functional data demonstrate the importance of charged side chains (Figure 3B). However, the energetic importance of Ile467 and Phe412 for the EGFR interaction suggests that binding is not driven by purely charged or polar interactions. Overall, the structural and alanine scanning results demonstrate that the dual-specific DL11 Fab engages distinct epitopes on the two receptors in a highly specific manner by unique use of light- and heavy-chain CDR residues.

MEHD7945A Potently Inhibits Receptor Phosphorylation of EGFR and HER3

We next evaluated the dual activity of MEHD7945A in cell signaling assays. To assess the inhibitory function on HER3, we chose MCF-7 cells for which HRG treatment potently activates the HER2/HER3 pathway. Treatment with MEHD7945A prior to HRG stimulation potently inhibited the phosphorylation of HER3 in a dose-dependent manner, and markedly decreased the phosphorylation of AKT and ERK1/2 (Figure 4A). MEHD7945A inhibited phosphorylation of HER3 with an IC_{50} of 0.05 μg/ml, phosphorylation of AKT with an IC_{50} value of 0.19 μg/ml, and phosphorylation of ERK1/2 with an IC_{50} value of 1.13 μg/ml. Treatment with a monospecific antibody against HER3, anti-HER3, that has comparable binding affinity to HER3 (Table S1) achieved similar results. Anti-HER3 inhibited phosphorylation of HER3 with an IC_{50} of 0.12 μg/ml, phosphorylation of AKT with an IC_{50} value of 0.74 μg/ml, and phosphorylation of ERK1/2 with an IC_{50} value of 1.83 μg/ml. We pretreated EGFR-NR6 cells with MEHD7945A prior to ligand stimulation and determined that MEHD7945A inhibited phosphorylation of EGFR and ERK1/2 with IC_{50} values of 0.03 and 0.16 μg/ml, respectively (Figure 4B). The monospecific EGFR antibody cetuximab was

reference (gray). For HER3, the full-length version of HER3 ecd from PDB entry 1M6B is included for comparison (gray). The overall domain organization of HER3 1-513 is preserved from the full-length ecd, albeit imperfectly. There are 24 amino acids (Gly12–Glu36), which are present in our model but were not visible in 1M6B. These residues adopt a conformation closely similar to that of homologous residues in EGFR, HER2, and HER4.

(B) DL11 epitopes of aligned EGFR (left) and HER3 (right) domains 3. The surface colors are dark blue for the contact surface (4 Å cutoff), red for residues that are functionally critical, determined by mutagenesis (residues labeled in red) and gray elsewhere. For EGFR, a dashed line outlines the contact region (4 Å cutoff) for EGF from the PDB entry 1IVO.

(C) When viewed with superposed antigens (colored as in part A) it is apparent that DL11 (pink, represented by Tyr96 from the light chain for clarity) is shifted by 13 Å.

(D) Sequence alignment of the DL11 epitope regions on EGFR and HER3. Dots in green field denote EGFR residues within 4 Å of DL11. Dots in orange field denote HER3 residues within 4 Å of DL11. Murine ortholog and human HER2 sequences are provided for comparison. Amino acid code letters are colored according to side chain character. Boxed dots indicate functionally important residues colored red in part (B). Residue numbers appear in gray.

See also Figure S2 and Tables S3 and S4.

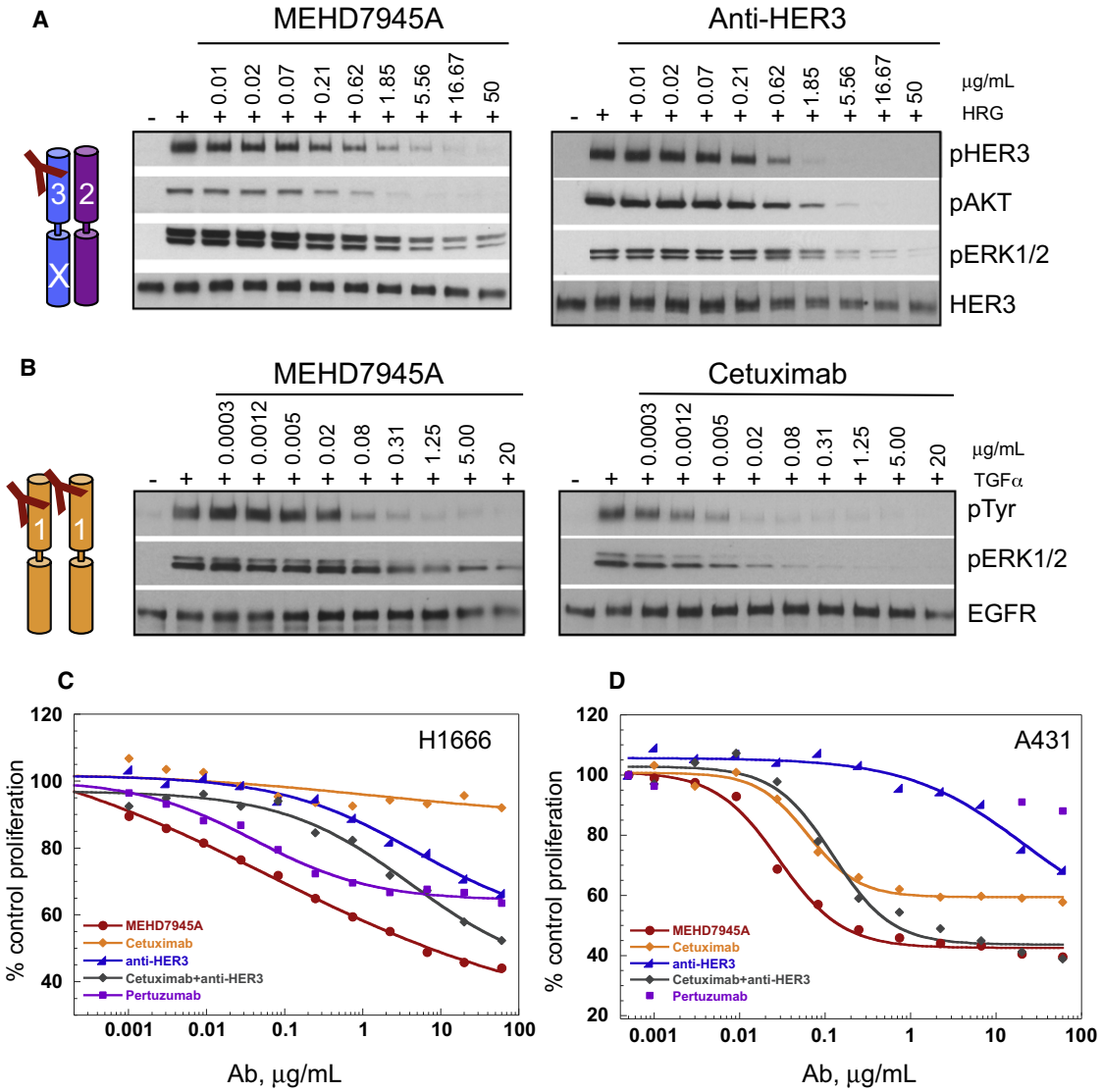

Figure 4. MEHD7945A Inhibits EGFR and HER2/HER3-Dependent Signaling

(A) MCF-7 cells treated with indicated concentrations of MEHD7945A or anti-HER3 were stimulated with 0.5 nM HRG for 10 min. Cell lysates were immunoblotted to detect pHER3 (Tyr1289), pAKT (Ser473), pERK1/2 (Thr202/Tyr204), and total HER3.

(B) EGFR-NR6 cells treated with indicated concentrations of MEHD7945A or cetuximab for 1 hr prior stimulation with 5 nM TGF-α for 10 min. Cell lysates were subjected to immunoblotting to detect, pERK1/2 (Thr202/Tyr204), total EGFR, and phosphorylated EGFR. Since EGFR-NR6 cells only express EGFR all potential phosphorylation sites of EGFR were detected using a pTyr antibody.

(C) H1666 cells were treated with increasing concentration of cetuximab (orange line), pertuzumab (purple line), anti-HER3 (blue line), the combination of cetuximab plus anti-HER3 (gray line) or MEHD7945A (red line) in the presence of HRG (2 nM). Concentrations shown on the x axis reflect the concentration of the single antibody. Cell proliferation relative to untreated control was measured after 4 days using AlamarBlue staining.

(D) A431 cells were treated with increasing concentrations of cetuximab (orange line), pertuzumab (purple dots), anti-HER3 (blue line), the combination of cetuximab plus anti-HER3 (gray line) or MEHD7945A (red line). Cell proliferation relative to untreated control was measured after 3 days using AlamarBlue staining.

See also Figure S3.

more effective in inhibiting phosphorylation of EGFR and downstream signaling molecules, which was likely due to the higher binding affinity to EGFR (Table S1). Moreover, betacellulin- and amphiregulin-induced EGFR phosphorylation was also inhibited by MEHD7945A (Figure S3). MEHD7945A inhibited ERK1/2 and AKT pathways as potently as the combination of anti-HER3 and cetuximab in A431 and BxPC3 cells (Figure S3).

Having established MEHD7945A as a potent inhibitor of ligand binding (Figure S3) and signaling, we next compared it to monospecific antibodies in cell proliferation assays. We first chose the NSCLC cell line H1666 that expresses EGFR, EGFR ligands, HER2, and HER3 (Zhou et al., 2006) and responds to HRG stimulation (Schaefer et al., 2007). For monospecific anti-HER antibodies, we chose cetuximab as an EGFR inhibitor,

pertuzumab as an HER2 inhibitor (Agus et al., 2002) and anti-HER3. Cetuximab did not significantly inhibit cell growth but a dose-dependent decrease of proliferation was seen with either pertuzumab or anti-HER3 (Figure 4C). The greatest inhibition of cell growth, however, was achieved with MEHD7945A, suggesting that inhibition of both EGFR and HER3 is more efficacious in cells where both receptors are prone to activation. Intriguingly, MEHD7945A potently inhibited cell proliferation at lower antibody concentrations compared with the combination of cetuximab plus anti-HER3. The greater potency may be due to MEHD7945A's unique ability to simultaneously engage two EGFR, two HER3 or one of each receptor on the surface of cells. We performed similar proliferation assays using A431 cells that do not require exogenous ligands for growth. MEHD7945A also inhibited the proliferation of these cells more potently than cetuximab, pertuzumab, anti-HER3, and also the combination of cetuximab plus anti-HER3 (Figure 4D). Taken together, these data demonstrate that MEHD7945A exhibits increased antiproliferative activity compared with monospecific HER antibodies in vitro.

MEHD7945A Inhibits HER3-Dependent Cell Growth In Vitro and In Vivo

To identify HER3-driven tumors in which to examine the in vivo activity of MEHD7945A, we performed an RNAi screen. Knockdown of receptor expression was confirmed by immunoblotting. BxPC3, a pancreatic cancer cell line, showed the strongest growth inhibitory effect upon HER3 silencing. RNAi knockdown of EGFR also slowed the growth of BxPC3 cells but to a lesser extent suggesting growth of BxPC3 cells was mainly mediated by HER3 and only in part by EGFR (Figure 5A).

We next determined the growth inhibitory effect of anti-HER3 and MEHD7945A in BxPC3 cells. HRG-stimulated cells were treated with anti-HER3, pertuzumab, cetuximab, or MEHD7945A. As expected, treatment with anti-HER3 had a strong antiproliferative effect (IC_{50} = 1.10 μg/ml), whereas pertuzumab only slightly inhibited growth and cetuximab was not effective under these conditions (Figure 5B). MEHD7945A was superior to all other treatments and inhibited growth of BxPC3 cells with an IC_{50} value of 0.01 μg/ml.

To test MEHD7945A activity in vivo, BxPC3 cells were injected subcutaneously into C.B-17 SCID mice and established tumors were treated once a week with MEHD7945A, pertuzumab, cetuximab, or anti-HER3. Because of its shorter half-life, we adjusted the dosing of anti-HER3 to achieve an exposure similar to the other antibodies. MEHD7945A inhibited tumor growth by 67% compared with vehicle control (Figure 5C). Anti-HER3 suppressed tumor growth by 37%, whereas pertuzumab and cetuximab had only marginal effects. Tumor lysates were collected 24 hr posttreatment and we verified that MEHD7945A markedly decreased the phosphorylation of HER3 (Figure 5C). To further investigate and compare the potency of MEHD7945A and anti-HER3, we considered a patient-derived human breast cancer transplant model, MAXF449. Established tumors were treated once a week with MEHD7945A, pertuzumab, cetuximab, anti-HER3, or the combination of cetuximab plus anti-HER3. MEHD7945A and anti-HER3 significantly suppressed tumor growth by 87% and 86%, respectively, whereas cetuximab had no effect (Figure 5D).

MEHD7945A Shows Increased Activity in Xenografts Relative to the Respective Monospecific Antibodies

We next investigated the effect of MEHD7945A on EGFR-dependent tumor growth using the NSCLC model NCI-H292. Complete tumor regression was seen in both dose groups of MEHD7945A (6.25 and 12.5 mg/kg) and in the 12.5 mg/kg cetuximab control group suggesting that the dual-specific antibody was as effective as cetuximab. The anti-HER3 antibody, as expected, did not have a statistically significant effect despite administration of a high dose (Figure 6A). Tumor lysates were collected 24 hr posttreatment and we verified that MEHD7945A markedly decreased the phosphorylation of EGFR and the downstream molecules phospho-ERK1/2 and phospho-S6 ribosomal protein (Figure 6A).

Next, we determined the activity of MEHD7945A relative to monospecific antibodies in additional xenografts where both EGFR and HER3 signaling contribute to tumor growth. The tumor growth of Calu-3 xenografts (NSCLC) was inhibited by cetuximab (tumor growth inhibition: TGI 17%) or the anti-HER3 antibody (TGI 33%), while the combined blockade of EGFR- and HER3-mediated signaling by MEHD7945A was most effective in inhibiting tumor growth (TGI 56%) (Figure 6B). A similar antitumor effect was seen when cetuximab and anti-HER3 were given in combination (TGI 56%). Greater activity of MEHD7945A compared with monospecific antibodies was also seen in the FaDu (head and neck squamous cell carcinoma) xenograft model. Interestingly, anti-HER3 and MEHD7945A were equally potent during the course of antibody treatment, whereas pertuzumab had no effect. However, the effect of MEHD7945A was more sustained posttreatment compared with anti-HER3 or cetuximab treatment (Figure 6C). Table S5 summarizes the in vivo potency of MEHD7945A compared with monospecific antibodies in numerous murine xenograft models. Collectively, MEHD7945A had equal activity to a monospecific EGFR antibody when tumor growth is dependent on EGFR and similar to a monospecific HER3 antibody when tumor growth depended on HER3 activation. However, when both receptors contributed to tumor growth MEHD7945A showed superior efficacy over monospecific antibodies. These results confirm our hypothesis that blocking more than one HER receptor pair (EGFR homo/heterodimers and HER3/HER2 heterodimers) substantially increases efficacy in HER-dependent tumors.

MEHD7945A Enhances Gemcitabine-Mediated Cytotoxicity In Vitro and In Vivo

We investigated whether the combination of MEHD7945A and gemcitabine, a chemotherapeutic agent commonly used in NSCLC, would enhance the inhibition of cell proliferation of MEHD7945A sensitive cell lines. NCI-H292, NCI-H1666, H358, and HCC827 were treated with MEHD7945A plus gemcitabine over a wide range of drug concentrations. Cell growth data were analyzed using CalcuSyn software (Chou and Talalay, 1984). The resulting combination index (C.I.) values were <1 for most of the effective range of the drugs (fractional effect 0.2–0.8), demonstrating that the combination inhibited proliferation synergistically in these cell lines (Figure 6D).

We further evaluated combination treatment of gemcitabine and MEHD7945A in vivo. NCI-H1975 tumors were treated with gemcitabine (100 mg/kg biweekly), a moderately efficacious

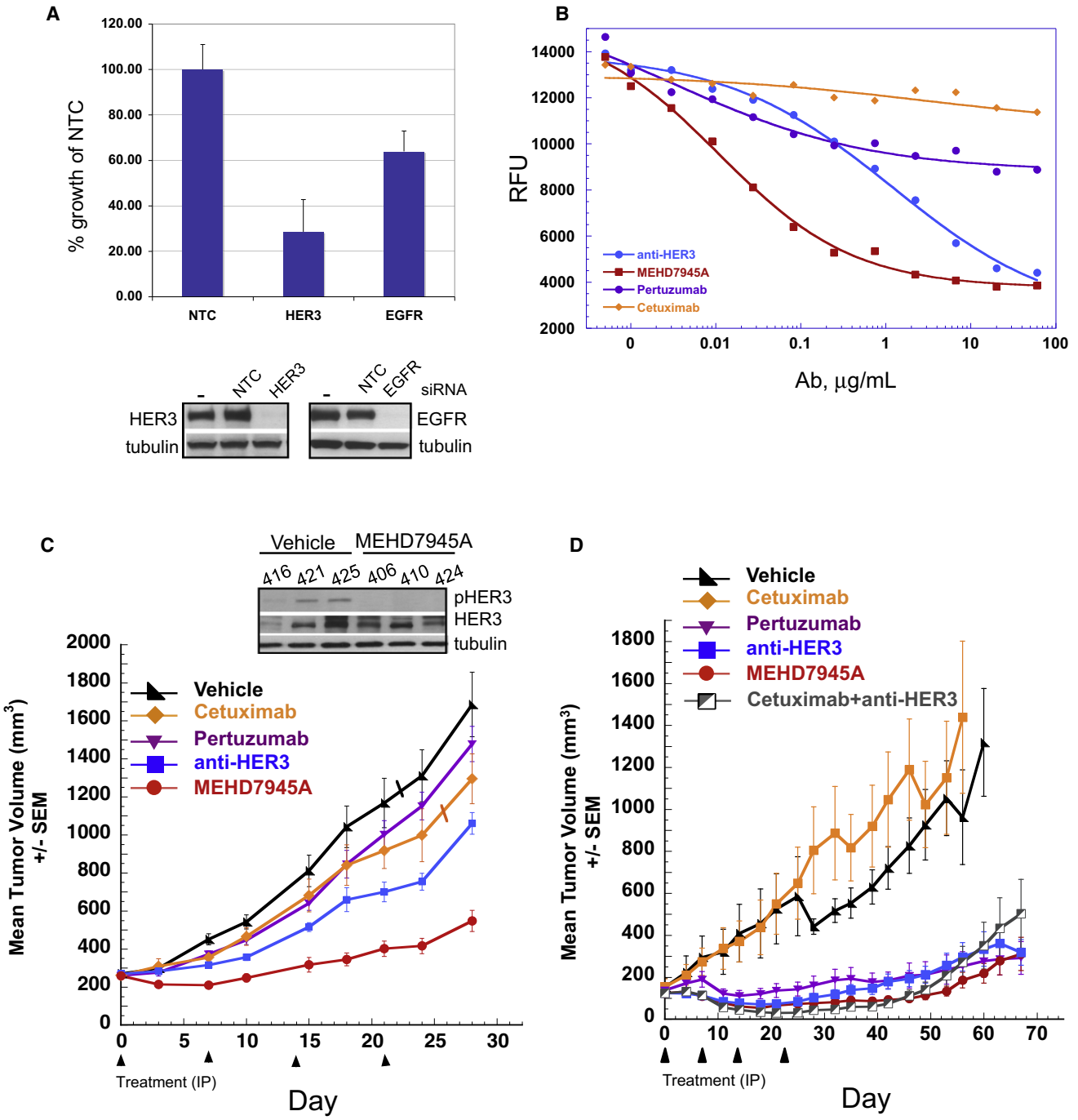

Figure 5. BxPC3 Cells and Xenografts Are Dependent on HER3 Signaling

(A) Knockdown of HER3 or EGFR by siRNA changes growth rate of BxPC3. Data presented as percentage of control cell growth. Error bars represent ± SD. Detection of HER3 or EGFR levels after siRNA treatment in BxPC3 cells by immunoblotting.

(B) BxPC3 cells were treated with indicated concentrations of anti-HER3 (blue), MEHD7945A (red), pertuzumab (purple), or cetuximab (orange) and cell proliferation was analyzed after 4 days by AlamarBlue staining.

(C) BxPC3 tumor-bearing mice were treated weekly using pertuzumab (25 mg/kg, purple line), cetuximab (25 mg/kg, orange line), anti-HER3 (50 mg/kg, blue line), MEHD7945A (25 mg/kg, red line), or vehicle (black line). First dose was given as a 2× loading dose. Arrows indicate treatments and data are presented as mean tumor volume ± SEM. Percent tumor growth inhibition (TGI) was evaluated at Day 28. Tumor lysates of vehicle or MEHD7945A (25 mg/kg) treated tumors were generated 24 hr posttreatment and phosphoHER3 status analyzed by immunoblotting.

(D) MAXF449 tumor-bearing mice were weekly injected intravenously with cetuximab (30 mg/kg, orange line), anti-HER3 (60 mg/kg, blue line), MEHD7945A (30 mg/kg, red line), vehicle (black line), or intraperitoneally with pertuzumab (30 mg/kg, purple line). First dose was given as a 2× loading dose. Arrows indicate treatments and data are presented as mean tumor volume ± SEM. Percent tumor growth inhibition (TGI) was evaluated at Day 25.

dose of MEHD7945A (2 mg/kg, weekly) or the combination thereof. Adding a chemotherapeutic agent to the dual-specific antibody resulted in strong tumor regression, whereas single agents led to only delayed tumor growth (Figure 6E).

MEHD7945A Mediates Antibody-Dependent Cell-Mediated Cytotoxicity

Clinical and preclinical data from monoclonal antibodies such as rituximab and trastuzumab (Junttila et al., 2010; Robak, 2009) indicate that antibody-dependent cell-mediated cytotoxicity (ADCC) contributes to their activities. In vitro and in vivo studies imply that ADCC is at least partly involved in the antitumor activity of cetuximab (Taylor et al., 2009). We therefore sought to determine if MEHD7945A induces ADCC in vitro. A431 cells were incubated with freshly isolated human peripheral blood mononuclear cells (PBMCs) in the presence of MEHD7945A, cetuximab, anti-HER3, or control antibody. MEHD7945A as well as cetuximab mediated strong cytolytic activity, whereas anti-HER3 or control antibody did not (Figure 7A).

To investigate the contribution of ADCC to the in vitro and in vivo activity of MEHD7945A, we introduced the previously characterized N297A mutation into the Fc domain of MEHD7945A (Presta, 2006). ADCC is triggered when an antibody binds to its antigen on a target cell and via its Fc region engages Fcγ receptors that are expressed on immune effector cells. The N297A mutation severely compromises the antibody's ability to recruit immune effector cells. Indeed, MEHD7945A_N297A (designated MEHD_N297A) was unable to induce ADCC of NCI-H292 cells, whereas MEHD7945A provided a strong ADCC response (Figure 7B). The N297A mutation did not affect the antiproliferative activity of the antibody. MEHD_N297A was as potent as MEHD7945A in inhibiting cell growth in vitro (data not shown).

We next examined if ADCC also played a significant role in the efficacy of MEHD7945A in vivo. We used the NCI-H292 EGFR-dependent xenograft model to compare the efficacy of MEHD7945A and its variant MEHD_N297A. Interestingly, both antibodies showed comparable activity through day 7 suggesting that treatment with either antibody led to reduced tumor volume by blocking the EGFR signaling pathway. However, when antibody concentrations lessened over time MEHD7945A sustained its in vivo potency for a much longer period than did MEHD_N297A (Figure 7C). Since antibody exposure levels were equal (data not shown), we attributed the difference in potency to the fact that MEHD7945A was able to engage immune effector cells but MEHD_N297A was not. A similar dual mode of action involving inhibition of signaling and ADCC was recently described for other anti-EGFR antibodies (Bleeker et al., 2004; Schneider-Merck et al., 2010).

MEHD7945A Administration to Cynomolgus Monkeys Results in Reduced Skin Toxicity Compared with Cetuximab

In a majority of patients, the administration of EGFR antagonists causes dermatologic toxicity that can become severe enough to require dose reduction or drug discontinuation (Li and Perez-Soler, 2009). To investigate if simultaneous inhibition of HER3 influences this adverse event, we compared the relative dermatologic toxicity of MEHD7945A to cetuximab. Female cynomolgus monkeys (three/group) were administered either cetuximab (25 mg/kg weekly) or MEHD7945A (at 25 mg/kg or 12.5 mg/kg weekly) intravenously for 5 weeks. As summarized in Table 1 and consistent with prior reports, dermatologic toxicity was observed between the third and fourth doses in all three cetuximab-treated animals (available at http://www.accessdata.fda.gov/drugsatfda_docs/bla/2004/125084_ERBITUX_PHARMR_P1.PDF). In contrast, only one of three animals given MEHD7945A at 25 mg/kg had evidence of dermatologic toxicity. Notably, the skin lesions were of lesser extent and severity, compared with the skin lesions in animals given cetuximab, and appeared only after the sixth dose. No animals treated with 12.5 mg/kg of MEHD7945A had any gross evidence of dermatologic toxicity. Pharmacokinetic analysis confirmed comparable exposure between treatment groups dosed with cetuximab and MEHD7945A at 25 mg/kg (data not shown); thus, the reduced relative toxicity was not due to differential drug exposure. These data demonstrate that the dermatologic toxicity of MEHD7945A is substantially less than that of cetuximab and suggests that MEHD7945A may have a superior clinical safety profile in comparison to established EGFR antagonists.

DISCUSSION

Herein, we provide evidence that MEHD7945A is capable of binding two EGFR, two HER3, or one EGFR and one HER3 at the same time. Different from bispecific agents with two distinct monospecific binding functions, the presence of two identical Fab arms in MEHD7945A raises the possibility that for a given receptor density, any combination of EGFR and HER3 levels should be recognized with near-equivalent avidity.

We demonstrated the advantage of dual blockade to inhibit diverse intracellular signals in a number of in vitro systems and we showed significant tumor growth inhibition in 12 xenograft models that represent six different types of solid tumors. Interestingly, MEHD7945A is more active than the prototypical EGFR antibody, cetuximab, in four models, more active than our HER3 antibody in five models, and is equivalently efficacious as cetuximab or our HER3 antibody in the remaining three models. Other investigators have recently reported on the identification, characterization, and initial clinical assessment of specific HER3 antibodies. To date, the most extensively characterized HER3 antibody is MM-121 (Schoeberl et al., 2010). Notably, MM-121 is engineered as an IgG2, which is not expected to efficiently bind to FcγRIIIa on human immune effector cells (Gessner et al., 1998). As such, MM-121 will not mediate antibody-dependent cell-mediated cytotoxicity (ADCC). In contrast, we show both in vitro and in vivo that MEHD7945A, as an IgG1, is highly effective in facilitating ADCC. Because MM-121 was not available for direct comparison, we tested MEHD7945A in the A549 NSCLC model that has also been studied with MM-121. A549 tumors were sensitive to anti-HER3 therapy with both our dual-specific and monospecific HER3-directed agents. Interestingly, similar efficacy was achieved with MEHD7945A dosed at 100 mg/kg for 3 weeks as when MM-121 was dosed at 210 mg/kg for 3 weeks (Schoeberl et al., 2009). We acknowledge the limitations of this comparison. Nevertheless, it is plausible that the increased potency observed with MEHD7945A is due to slower clearance, targeting of both

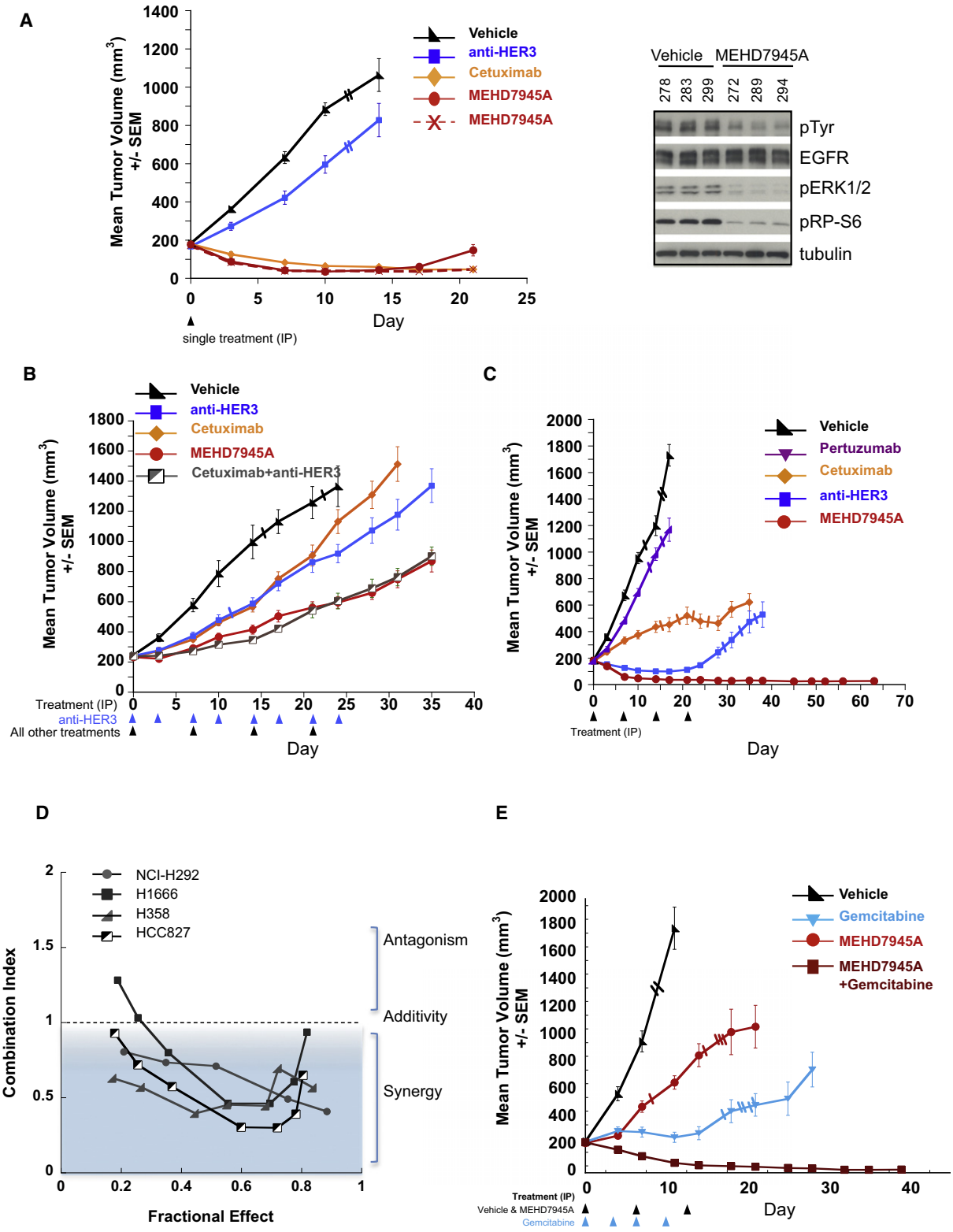

Figure 6. MEHD7945A Inhibits Tumor Growth in Xenograft Models and Shows Increased Inhibition When Combined with Gemcitabine

(A) Mice with established NCI-H292 xenografts were injected intraperitoneally with single dose of anti-HER3 (100 mg/kg, blue line), cetuximab (12.5 mg/kg, orange line), MEHD7945A (6.25 mg/kg, red line), MEHD7945A (12.5 mg/kg, red dashed line), or vehicle (black line). Data are presented as mean tumor volume ± SEM. Tumor lysates from vehicle or MEHD7945A (single dose, 50 mg/kg) treated tumors were generated 24 hr posttreatment and analyzed for phospho EGFR using a pTyr antibody, pERK1/2 (Thr202/Tyr204), p-S6 ribosomal protein (pRP-S6; Ser235/236), EGFR, and tubulin.

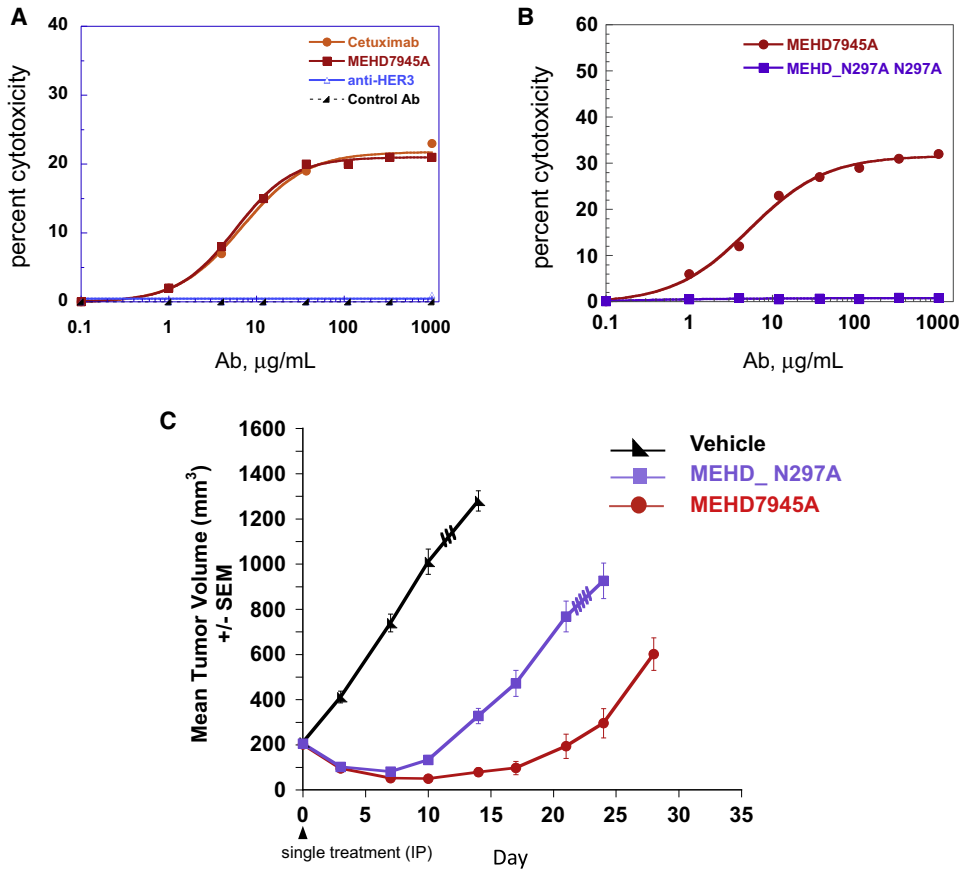

Figure 7. ADCC Contributes to the Antitumor Efficacy of MEHD7945A

(A) EGFR amplified A431 cells with normal expression of HER3 were incubated with freshly isolated PBMCs at a ratio of 1:25 and indicated concentrations of cetuximab, MEHD7945A, anti-HER3, or control antibody. Antibody-dependent cytotoxicity was determined by measuring lactate dehydrogenase (LDH) release in the supernatant.

(B) NCI-H292 cells and freshly isolated PBMCs (1:25 ratio) were incubated with indicated concentrations of MEHD7945A or MEHD7945A_N297A (in figure abbreviated to MEHD_N297A), and LDH release was determined in the supernatant.

(C) NCI-H292-bearing mice were treated with a single dose of MEHD7945A (6.25 mg/kg, red line), MEHD7945A_N297A (6.25 mg/kg, purple line), or vehicle (black line), and data are presented as mean tumor volume ± SEM.

HER3 and EGFR, engagement of immune effector functions, or a combination of some or all of these attributes.

We hypothesized that given HER3's ability to potently couple to the PI3 kinase pathway, antagonizing HER signaling with our dual-targeted agent in the presence of chemotherapy may broadly potentiate cytotoxicity. Our initial investigations suggest that the cytotoxicity of gemcitabine is strongly augmented by MEHD7945A (Figure 6). Significantly greater in vivo activity was seen in the NCI-1975 NSCLC model, whose EGFR harbors both an activating mutation (L858R) and the erlotinib/gefitinib resistance mutation (T790M). These data are particularly intriguing since large clinical trials of chemotherapy in combination with erlotinib or gefitinib in lung cancer were unsuccessful (Giaccone, 2004; Herbst et al., 2005).

(B) Calu-3-bearing mice were treated weekly with cetuximab (25 mg/kg, orange line), MEHD7945A (25 mg/kg, red line), biweekly with anti-HER3 (25 mg/kg, blue line), the combination of weekly cetuximab + biweekly anti-HER3 (25 mg/kg each), gray line), or vehicle (black line). First dose was given as a 2× loading dose. Arrows indicate treatments and data are presented as mean tumor volume ± SEM. Percent TGI was evaluated at Day 24.

(C) FaDu tumor-bearing mice were treated weekly with cetuximab (25 mg/kg, orange line), pertuzumab (25 mg/kg, purple line), MEHD7945A (25 mg/kg, red line), anti-HER3 (50 mg/kg, blue line), or vehicle (black line). First dose was given as a 2× loading dose. Cross bars indicate euthanized animals. Arrows indicate days of dosing and data are presented as mean tumor volume ± SEM

(D) Cell proliferation of NCI-H292, H1666, H358, and HCC827 cells was determined after 5 days of treatment with MEHD7945A and gemcitabine. Combination index (C.I.) values were determined using CalcuSyn software. For drug combinations with fractional effect between 0.2 and 0.8 (inhibiting 20%–80% of proliferation) C.I. values <1 indicate drug synergy.

(E) NCI-H1975-bearing mice were treated weekly with MEHD7945A (2 mg/kg, red line), biweekly with gemcitabine (100 mg/kg, blue line), the combination of weekly MEHD7945A+ biweekly gemcitabine (brown line) or vehicle (black line). Cross bars indicate euthanized animals. Arrows indicate treatments and data are presented as mean tumor volume ± SEM. Percent TGI was evaluated at Day 25. See also Table S5.

Table 1. Preclinical Toxicology Results from Nonhuman Primates

		Dermatological Findings	
Test Article[a]	Dose (mg/kg)[b]	Time to Onset (Study Day)	Extent and Severity
Cetuximab	25	16, 19, 22[c]	Mild to Severe[d]
MEHD7945A	25	43, NA, NA	Mild to Moderate
MEHD7945A	12.5	NA, NA, NA	NA

NA, not applicable.
[a] Cynomolgus monkeys (n = 3/group) were given cetuximab or MEHD7945A weekly for 5 weeks (total of six doses) followed by a 4 week recovery period.
[b] Drug exposure was comparable for cetuximab and MEHD7945A given at 25 mg/kg throughout the study period.
[c] Time to onset of dermatologic lesions is comparable to those previously reported for cetuximab (available at http://www.accessdata.fda.gov/drugsatfda_docs/bla/2004/125084_ERBITUX_PHARMR_P1.PDF).
[d] Dermatological lesions remained throughout drug administration phase and resolved by the end of the 4 week drug-free recovery period (Study Day 63).

Unexpectedly, our nonhuman primate studies revealed that MEHD7945A exhibits far less skin toxicity in comparison to cetuximab. Evidently, simultaneous blockade of HER3 and EGFR signaling does not worsen the well-known skin liability of established EGFR antagonists and appears to decrease their dermatologic toxicity. The mechanistic explanation for this observation is currently under investigation. One plausible hypothesis is that heregulin-HER3 signaling in the skin is a stress response to EGFR antagonism. Naturally, confirmation of this observation awaits validation in human subjects.

In contrast to EGFR or HER2, no prevalent genetic alterations are reported for HER3. As a result, cancer patients whose tumors are driven by HER3 activation may be difficult to identify due to technical complexities in analyzing pathway activation in archival tumor tissue. Here, we demonstrated that TGF-α predominantly activated the MAPK pathway in both normal and EGFR-amplified cells, whereas HRG stimulation of HER3 primarily activated the PI3K/AKT pathway, and only blockade of both EGFR and HER3 signaling completely ablated activation of both pathways under ligand-rich conditions. These data are in agreement with clinical observations of strong downmodulation of MAPK signaling but not AKT signaling in skin and tumor biopsies of patients treated with anti-EGFR agents (Folprecht et al., 2008; Tabernero et al., 2010). Recent diagnostic studies underscore the interplay of EGFR, HER3, and their ligands in HNSCC (Hickinson et al., 2009).

Sensitivity to a particular anticancer agent evolves during treatment (Engelman and Settleman, 2008; Wheeler et al., 2008). It is plausible that simultaneously targeting of more than one proliferation and survival signal, or targeting a resistance mechanism, will provide better clinical outcomes. The interdependence of HER/ErbB receptors may underlie acquired resistance to EGFR or HER2 targeted agents. A variety of compensatory mechanisms are postulated: upregulation of ligands for HER3 or EGFR (Kong et al., 2008; Yonesaka et al., 2011; Zhou et al., 2006), switching dimerization partners (Jain et al., 2010), or overexpression of receptors, especially HER3 (Campbell et al., 2010; Ritter et al., 2007). Because HER3 activation and/or expression are identified as an evolved response to current anti-HER/ErbB agents, early and direct blockade of HER3 signaling may delay drug resistance. Recent data in support of this hypothesis were obtained in a genetically engineered mouse model of lung cancer demonstrating that cetuximab treatment results in the upregulation of HER3 phosphorylation and HRG expression and combined treatment with cetuximab and the HER3 antibody MM-121 delays resistance (Schoeberl et al., 2010).

Taken together, there is accumulating evidence to support the hypothesis that simultaneously targeting more than one proliferation and survival signal, or targeting a resistance mechanism, will provide better clinical outcomes. The unique potential of MEHD7945A to both treat EGFR/HER3-driven disease and delay HER3-dependent drug resistance warrants its consideration as a promising anticancer therapy in the clinic.

EXPERIMENTAL PROCEDURES

Phage Library Construction and Selection

Phage-displayed Fab libraries with randomized heavy-chain CDRs were constructed as previously described with modestly modified degenerate oligonucleotides (Lee et al., 2004). To select EGFR binding clones, the libraries were subjected to four selection rounds on the immobilized target (EGFR-ECD-Fc). Random clones were screened for EGFR-specific binders using ELISA (Lee et al., 2004). The relative binding affinity was determined by competitive phage ELISA. In short, purified phage clones that gave a 50%–70% saturating signal were incubated with increasing concentrations of antigen (hEGFR-ECD) for 1 hour and unbound phage was captured in antigen-coated ELISA wells and detected using an anti-phage antibody. EC_{50} was calculated as the concentration of antigen in solution that inhibited 50% of the phage from binding to immobilized antigen. To recruit a second binding specificity into D1.5, selected light-chain CDRs of D1.5 Fab displayed on phage were mutated (Bostrom et al., 2009). The libraries were subjected to four rounds of binding selection for HER3 and screening as described for the heavy-chain libraries. Clones that bound HER3 in addition to EGFR were identified and expressed as Fab and IgG for further characterization.

Crystallization, Structure Determination, and Refinement

DL11 was produced in *Escherichia coli*. The HER3 ECD domains 1-3 (Ser1-His513) and EGFR ECD domain 3 (Arg310-Lys514) with C-terminal histidine affinity tags (-GNSHis$_6$) were each produced in baculovirus-infected insect cells. DL11 alone and its complexes with HER3 and EGFR fragments were subjected to crystallization trials in sitting drops. The sequence of DL11 differs from that of DL11f in only three places (Figure 2A). Detailed information from protein production, crystallization, and structure solution appears in Supplemental Material, including data reduction and refinement statistics in Table S3.

In Vivo Drug Efficacy

For xenograft studies, naive SCID beige or C.B-17 SCID mice (Charles River Laboratories, San Diego or Hollister, CA) were inoculated subcutaneously with Calu3, NCI-H292, BxPC3, NCI-H1975, or FaDu cells. Mice with similarly sized tumors (mean volume 150–350 mm^3) were randomized into treatment cohorts and treatments were administered intraperitoneally. Single-dose studies consisted of a single treatment on the day of randomization. Multiple-dose studies consisted of 4 weeks of treatment, with the first dose (day of randomization) being a 2× loading dose. Tumors were measured with calipers at least once a week. Studies were reviewed and approved by the Institutional Animal Care and Use Committee (IACUC) at Genentech. The MAXF449 xenograft model was established at Oncotest GmbH from primary patient material after informed consent of the patient and approval by the Ethics Board at the University of Freiburg. The mouse efficacy experiment was reviewed and approved by the Regierungs präsidium Freiburg, Germany, and conducted according to the guidelines of the German Animal Welfare Act. Xenografts were subcutaneously grown in athymic NMRI nu/nu mice and

randomized after reaching tumor volumes of 100 mm^3. Mice were treated with antibodies once a week intravenously with the exception of pertuzumab, which was administered intraperitoneally. Antibodies were dosed for 4 consecutive weeks with the first dose (day of randomization) being a 2× loading dose.

Toxicity Study in Cynomolgus Monkeys

Nine experimentally naive female cynomolgus monkeys (*Macaca fascicularis*) were randomly assigned to dosing groups (n = 3/group). Cetuximab (Capital Wholesale Drug Company) was not diluted prior to dose administration and used at the supplied concentration. Dilutions of MEHD7945A to 5 or 2.5 mg/ml were performed on each dosing day. Cetuximab (Group 1; 25 mg/kg) or MEHD7945A (Groups 2 and 3; 25 mg/kg and 12.5 mg/kg, respectively) was administered via slow pump infusion once weekly for six doses over 5 consecutive weeks (Days 1, 8, 15, 22, 29, and 36). Cage-side observations were performed once daily during acclimation and twice daily beginning on Day 1. Each animal was observed for overall health, including evidence of dermatologic toxicity. All animals were housed, maintained, and treated in accordance to standard ethical animal handling guidelines. The study was reviewed and approved by the Institutional Animal Care and Use Committee (IACUC) at Valley Biosystems.

ACCESSION NUMBERS

Final refined coordinates and structure factors for DL11 alone and its complexes with EGFR and HER3 have been deposited at the Protein Data Bank under accession codes 3P0V, 3P0Y, and 3P11, respectively.

Supplemental Material

Supplemental Material includes Experimental Procedures, references, three figures, and five tables and can be found online at doi:10.1016/j.ccr.2011.09.003.

ACKNOWLEDGMENTS

We are grateful to S. Murli, K. Billeci, R. Akita, L. Berry, W. Halpern, and R. Iyer for critical reagents and discussions. M. Ultsch, J. Murray, K. Dong, and W. Wang collected diffraction data. Portions of this research were conducted at the Advanced Light Source and at the Stanford Synchrotron Radiation Lightsource, which are operated on behalf of the U.S. Department of Energy, Office of Basic Energy Sciences.

Received: October 18, 2010
Revised: June 17, 2011
Accepted: September 9, 2011
Published: October 17, 2011

REFERENCES

Agus, D.B., Akita, R.W., Fox, W.D., Lewis, G.D., Higgins, B., Pisacane, P.I., Lofgren, J.A., Tindell, C., Evans, D.P., Maiese, K., et al. (2002). Targeting ligand-activated ErbB2 signaling inhibits breast and prostate tumor growth. Cancer Cell *2*, 127–137.

Bleeker, W.K., Lammerts van Bueren, J.J., van Ojik, H.H., Gerritsen, A.F., Pluyter, M., Houtkamp, M., Halk, E., Goldstein, J., Schuurman, J., van Dijk, M.A., et al. (2004). Dual mode of action of a human anti-epidermal growth factor receptor monoclonal antibody for cancer therapy. J. Immunol. *173*, 4699–4707.

Bostrom, J., Yu, S.F., Kan, D., Appleton, B.A., Lee, C.V., Billeci, K., Man, W., Peale, F., Ross, S., Wiesmann, C., and Fuh, G. (2009). Variants of the antibody herceptin that interact with HER2 and VEGF at the antigen binding site. Science *323*, 1610–1614.

Buck, E., Eyzaguirre, A., Haley, J.D., Gibson, N.W., Cagnoni, P., and Iwata, K.K. (2006). Inactivation of Akt by the epidermal growth factor receptor inhibitor erlotinib is mediated by HER-3 in pancreatic and colorectal tumor cell lines and contributes to erlotinib sensitivity. Mol. Cancer Ther. *5*, 2051–2059.

Campbell, M.R., Amin, D., and Moasser, M.M. (2010). HER3 comes of age: new insights into its functions and role in signaling, tumor biology, and cancer therapy. Clin. Cancer Res. *16*, 1373–1383.

Carraway, K.L., 3rd, Sliwkowski, M.X., Akita, R., Platko, J.V., Guy, P.M., Nuijens, A., Diamonti, A.J., Vandlen, R.L., Cantley, L.C., and Cerione, R.A. (1994). The erbB3 gene product is a receptor for heregulin. J. Biol. Chem. *269*, 14303–14306.

Chames, P., and Baty, D. (2009). Bispecific antibodies for cancer therapy. Curr. Opin. Drug Discov. Devel. *12*, 276–283.

Cho, H.S., and Leahy, D.J. (2002). Structure of the extracellular region of HER3 reveals an interdomain tether. Science *297*, 1330–1333.

Chou, T.C., and Talalay, P. (1984). Quantitative analysis of dose-effect relationships: the combined effects of multiple drugs or enzyme inhibitors. Adv. Enzyme Regul. *22*, 27–55.

Ciardiello, F., and Tortora, G. (2008). EGFR antagonists in cancer treatment. N. Engl. J. Med. *358*, 1160–1174.

Engelman, J.A., and Settleman, J. (2008). Acquired resistance to tyrosine kinase inhibitors during cancer therapy. Curr. Opin. Genet. Dev. *18*, 73–79.

Engelman, J.A., Jänne, P.A., Mermel, C., Pearlberg, J., Mukohara, T., Fleet, C., Cichowski, K., Johnson, B.E., and Cantley, L.C. (2005). ErbB-3 mediates phosphoinositide 3-kinase activity in gefitinib-sensitive non-small cell lung cancer cell lines. Proc. Natl. Acad. Sci. USA *102*, 3788–3793.

Folprecht, G., Tabernero, J., Köhne, C.H., Zacharchuk, C., Paz-Ares, L., Rojo, F., Quinn, S., Casado, E., Salazar, R., Abbas, R., et al. (2008). Phase I pharmacokinetic/pharmacodynamic study of EKB-569, an irreversible inhibitor of the epidermal growth factor receptor tyrosine kinase, in combination with irinotecan, 5-fluorouracil, and leucovorin (FOLFIRI) in first-line treatment of patients with metastatic colorectal cancer. Clin. Cancer Res. *14*, 215–223.

Gessner, J.E., Heiken, H., Tamm, A., and Schmidt, R.E. (1998). The IgG Fc receptor family. Ann. Hematol. *76*, 231–248.

Giaccone, G. (2004). The role of gefitinib in lung cancer treatment. Clin. Cancer Res. *10*, 4233s–4237s.

Grothey, A. (2010). EGFR antibodies in colorectal cancer: where do they belong? J. Clin. Oncol. *28*, 4668–4670.

Herbst, R.S., Prager, D., Hermann, R., Fehrenbacher, L., Johnson, B.E., Sandler, A., Kris, M.G., Tran, H.T., Klein, P., Li, X., et al; TRIBUTE Investigator Group. (2005). TRIBUTE: a phase III trial of erlotinib hydrochloride (OSI-774) combined with carboplatin and paclitaxel chemotherapy in advanced non-small-cell lung cancer. J. Clin. Oncol. *23*, 5892–5899.

Hickinson, D.M., Marshall, G.B., Beran, G.J., Varella-Garcia, M., Mills, E.A., South, M.C., Cassidy, A.M., Acheson, K.L., McWalter, G., McCormack, R.M., et al. (2009). Identification of biomarkers in human head and neck tumor cell lines that predict for in vitro sensitivity to gefitinib. Clin. Transl. Sci. *2*, 183–192.

Hynes, N.E., and MacDonald, G. (2009). ErbB receptors and signaling pathways in cancer. Curr. Opin. Cell Biol. *21*, 177–184.

Jain, A., Penuel, E., Mink, S., Schmidt, J., Hodge, A., Favero, K., Tindell, C., and Agus, D.B. (2010). HER kinase axis receptor dimer partner switching occurs in response to EGFR tyrosine kinase inhibition despite failure to block cellular proliferation. Cancer Res. *70*, 1989–1999.

Jones, R.B., Gordus, A., Krall, J.A., and MacBeath, G. (2006). A quantitative protein interaction network for the ErbB receptors using protein microarrays. Nature *439*, 168–174.

Junttila, T.T., Parsons, K., Olsson, C., Lu, Y., Xin, Y., Theriault, J., Crocker, L., Pabonan, O., Baginski, T., Meng, G., et al. (2010). Superior in vivo efficacy of afucosylated trastuzumab in the treatment of HER2-amplified breast cancer. Cancer Res. *70*, 4481–4489.

Jura, N., Endres, N.F., Engel, K., Deindl, S., Das, R., Lamers, M.H., Wemmer, D.E., Zhang, X., and Kuriyan, J. (2009a). Mechanism for activation of the EGF receptor catalytic domain by the juxtamembrane segment. Cell *137*, 1293–1307.

Jura, N., Shan, Y., Cao, X., Shaw, D.E., and Kuriyan, J. (2009b). Structural analysis of the catalytically inactive kinase domain of the human EGF receptor 3. Proc. Natl. Acad. Sci. USA *106*, 21608–21613.

Kong, A., Calleja, V., Leboucher, P., Harris, A., Parker, P.J., and Larijani, B. (2008). HER2 oncogenic function escapes EGFR tyrosine kinase inhibitors

via activation of alternative HER receptors in breast cancer cells. PLoS ONE *3*, e2881.

Lee, C.V., Hymowitz, S.G., Wallweber, H.J., Gordon, N.C., Billeci, K.L., Tsai, S.P., Compaan, D.M., Yin, J., Gong, Q., Kelley, R.F., et al. (2006). Synthetic anti-BR3 antibodies that mimic BAFF binding and target both human and murine B cells. Blood *108*, 3103–3111.

Lee, C.V., Liang, W.C., Dennis, M.S., Eigenbrot, C., Sidhu, S.S., and Fuh, G. (2004). High-affinity human antibodies from phage-displayed synthetic Fab libraries with a single framework scaffold. J. Mol. Biol. *340*, 1073–1093.

Li, S., Schmitz, K.R., Jeffrey, P.D., Wiltzius, J.J., Kussie, P., and Ferguson, K.M. (2005). Structural basis for inhibition of the epidermal growth factor receptor by cetuximab. Cancer Cell *7*, 301–311.

Li, T., and Perez-Soler, R. (2009). Skin toxicities associated with epidermal growth factor receptor inhibitors. Targeted Oncol. *4*, 107–119.

Lutterbuese, R., Raum, T., Kischel, R., Hoffmann, P., Mangold, S., Rattel, B., Friedrich, M., Thomas, O., Lorenczewski, G., Rau, D., et al. (2010). T cell-engaging BiTE antibodies specific for EGFR potently eliminate KRAS- and BRAF-mutated colorectal cancer cells. Proc. Natl. Acad. Sci. USA *107*, 12605–12610.

Lynch, D.H., and Yang, X.D. (2002). Therapeutic potential of ABX-EGF: a fully human anti-epidermal growth factor receptor monoclonal antibody for cancer treatment. Semin. Oncol. *29* (*Suppl 4*), 47–50.

Lynch, T.J., Bell, D.W., Sordella, R., Gurubhagavatula, S., Okimoto, R.A., Brannigan, B.W., Harris, P.L., Haserlat, S.M., Supko, J.G., Haluska, F.G., et al. (2004). Activating mutations in the epidermal growth factor receptor underlying responsiveness of non-small-cell lung cancer to gefitinib. N. Engl. J. Med. *350*, 2129–2139.

Moasser, M.M. (2007). Targeting the function of the HER2 oncogene in human cancer therapeutics. Oncogene *26*, 6577–6592.

Olayioye, M.A., Neve, R.M., Lane, H.A., and Hynes, N.E. (2000). The ErbB signaling network: receptor heterodimerization in development and cancer. EMBO J. *19*, 3159–3167.

Paez, J.G., Janne, P.A., Lee, J.C., Tracy, S., Greulich, H., Gabriel, S., Herman, P., Kaye, F.J., Lindeman, N., Boggon, T.J., et al. (2004). EGFR mutations in lung cancer: correlation with clinical response to gefitinib therapy. Science *304*, 1497–1500.

Presta, L.G. (2006). Engineering of therapeutic antibodies to minimize immunogenicity and optimize function. Adv. Drug Deliv. Rev. *58*, 640–656.

Prigent, S.A., and Gullick, W.J. (1994). Identification of c-erbB-3 binding sites for phosphatidylinositol 3′-kinase and SHC using an EGF receptor/c-erbB-3 chimera. EMBO J. *13*, 2831–2841.

Ritter, C.A., Perez-Torres, M., Rinehart, C., Guix, M., Dugger, T., Engelman, J.A., and Arteaga, C.L. (2007). Human breast cancer cells selected for resistance to trastuzumab in vivo overexpress epidermal growth factor receptor and ErbB ligands and remain dependent on the ErbB receptor network. Clin. Cancer Res. *13*, 4909–4919.

Robak, T. (2009). GA-101, a third-generation, humanized and glyco-engineered anti-CD20 mAb for the treatment of B-cell lymphoid malignancies. Curr. Opin. Investig. Drugs *10*, 588–596.

Schaefer, G., Fitzpatrick, V.D., and Sliwkowski, M.X. (1997). Gamma-heregulin: a novel heregulin isoform that is an autocrine growth factor for the human breast cancer cell line, MDA-MB-175. Oncogene *15*, 1385–1394.

Schaefer, G., Shao, L., Totpal, K., and Akita, R.W. (2007). Erlotinib directly inhibits HER2 kinase activation and downstream signaling events in intact cells lacking epidermal growth factor receptor expression. Cancer Res. *67*, 1228–1238.

Schneider-Merck, T., Lammerts van Bueren, J.J., Berger, S., Rossen, K., van Berkel, P.H., Derer, S., Beyer, T., Lohse, S., Bleeker, W.K., Peipp, M., et al. (2010). Human IgG2 antibodies against epidermal growth factor receptor effectively trigger antibody-dependent cellular cytotoxicity but, in contrast to IgG1, only by cells of myeloid lineage. J. Immunol. *184*, 512–520.

Schoeberl, B., Faber, A.C., Li, D., Liang, M.C., Crosby, K., Onsum, M., Burenkova, O., Pace, E., Walton, Z., Nie, L., et al. (2010). An ErbB3 antibody, MM-121, is active in cancers with ligand-dependent activation. Cancer Res. *70*, 2485–2494.

Schoeberl, B., Pace, E.A., Fitzgerald, J.B., Harms, B.D., Xu, L., Nie, L., Linggi, B., Kalra, A., Paragas, V., Bukhalid, R., et al. (2009). Therapeutically targeting ErbB3: a key node in ligand-induced activation of the ErbB receptor-PI3K axis. Sci. Signal. *2*, ra31.

Sliwkowski, M.X., Schaefer, G., Akita, R.W., Lofgren, J.A., Fitzpatrick, V.D., Nuijens, A., Fendly, B.M., Cerione, R.A., Vandlen, R.L., and Carraway, K.L., 3rd. (1994). Coexpression of erbB2 and erbB3 proteins reconstitutes a high affinity receptor for heregulin. J. Biol. Chem. *269*, 14661–14665.

Soltoff, S.P., Carraway, K.L., 3rd, Prigent, S.A., Gullick, W.G., and Cantley, L.C. (1994). ErbB3 is involved in activation of phosphatidylinositol 3-kinase by epidermal growth factor. Mol. Cell. Biol. *14*, 3550–3558.

Tabernero, J., Cervantes, A., Rivera, F., Martinelli, E., Rojo, F., von Heydebreck, A., Macarulla, T., Rodriguez-Braun, E., Eugenia Vega-Villegas, M., Senger, S., et al. (2010). Pharmacogenomic and pharmacoproteomic studies of cetuximab in metastatic colorectal cancer: biomarker analysis of a phase I dose-escalation study. J. Clin. Oncol. *28*, 1181–1189.

Taylor, R.J., Chan, S.L., Wood, A., Voskens, C.J., Wolf, J.S., Lin, W., Chapoval, A., Schulze, D.H., Tian, G., and Strome, S.E. (2009). FcgammaRIIIa polymorphisms and cetuximab induced cytotoxicity in squamous cell carcinoma of the head and neck. Cancer Immunol. Immunother. *58*, 997–1006.

Wheeler, D.L., Huang, S., Kruser, T.J., Nechrebecki, M.M., Armstrong, E.A., Benavente, S., Gondi, V., Hsu, K.T., and Harari, P.M. (2008). Mechanisms of acquired resistance to cetuximab: role of HER (ErbB) family members. Oncogene *27*, 3944–3956.

Yonesaka, K., Zejnullahu, K., Okamoto, I., Satoh, T., Cappuzzo, F., Souglakos, J., Ercan, D., Rogers, A., Roncalli, M., Takeda, M., et al. (2011). Activation of ERBB2 signaling causes resistance to the EGFR-directed therapeutic antibody cetuximab. Sci. Transl. Med. *3*, 99ra86.

Zhou, B.B., Peyton, M., He, B., Liu, C., Girard, L., Caudler, E., Lo, Y., Baribaud, F., Mikami, I., Reguart, N., et al. (2006). Targeting ADAM-mediated ligand cleavage to inhibit HER3 and EGFR pathways in non-small cell lung cancer. Cancer Cell *10*, 39–50.